NASA/TM—2008-215443 AIAA–2008–4749

# Numerical Investigation of LO2 and LCH4 Storage Tanks on the Lunar Surface

*Stephen Barsi*
*National Center for Space Exploration Research, Cleveland, Ohio*

*Jeff Moder*
*Glenn Research Center, Cleveland, Ohio*

*Mohammad Kassemi*
*National Center for Space Exploration Research, Cleveland, Ohio*

December 2008

# NASA STI Program . . . in Profile

Since its founding, NASA has been dedicated to the advancement of aeronautics and space science. The NASA Scientific and Technical Information (STI) program plays a key part in helping NASA maintain this important role.

The NASA STI Program operates under the auspices of the Agency Chief Information Officer. It collects, organizes, provides for archiving, and disseminates NASA's STI. The NASA STI program provides access to the NASA Aeronautics and Space Database and its public interface, the NASA Technical Reports Server, thus providing one of the largest collections of aeronautical and space science STI in the world. Results are published in both non-NASA channels and by NASA in the NASA STI Report Series, which includes the following report types:

- TECHNICAL PUBLICATION. Reports of completed research or a major significant phase of research that present the results of NASA programs and include extensive data or theoretical analysis. Includes compilations of significant scientific and technical data and information deemed to be of continuing reference value. NASA counterpart of peer-reviewed formal professional papers but has less stringent limitations on manuscript length and extent of graphic presentations.

- TECHNICAL MEMORANDUM. Scientific and technical findings that are preliminary or of specialized interest, e.g., quick release reports, working papers, and bibliographies that contain minimal annotation. Does not contain extensive analysis.

- CONTRACTOR REPORT. Scientific and technical findings by NASA-sponsored contractors and grantees.

- CONFERENCE PUBLICATION. Collected papers from scientific and technical conferences, symposia, seminars, or other meetings sponsored or cosponsored by NASA.

- SPECIAL PUBLICATION. Scientific, technical, or historical information from NASA programs, projects, and missions, often concerned with subjects having substantial public interest.

- TECHNICAL TRANSLATION. English-language translations of foreign scientific and technical material pertinent to NASA's mission.

Specialized services also include creating custom thesauri, building customized databases, organizing and publishing research results.

For more information about the NASA STI program, see the following:

- Access the NASA STI program home page at *http://www.sti.nasa.gov*

- E-mail your question via the Internet to *help@sti.nasa.gov*

- Fax your question to the NASA STI Help Desk at 301–621–0134

- Telephone the NASA STI Help Desk at 301–621–0390

- Write to:
  NASA Center for AeroSpace Information (CASI)
  7115 Standard Drive
  Hanover, MD 21076–1320

NASA/TM—2008-215443 AIAA–2008–4749

# Numerical Investigation of LO2 and LCH4 Storage Tanks on the Lunar Surface

*Stephen Barsi*
*National Center for Space Exploration Research, Cleveland, Ohio*

*Jeff Moder*
*Glenn Research Center, Cleveland, Ohio*

*Mohammad Kassemi*
*National Center for Space Exploration Research, Cleveland, Ohio*

Prepared for the
44th Joint Propulsion Conference and Exhibit
cosponsored by AIAA, ASME, SAE, and ASEE
Hartford, Connecticut, July 21–23, 2008

National Aeronautics and
Space Administration

Glenn Research Center
Cleveland, Ohio 44135

December 2008

## Acknowledgments

This work was supported by the Cryogenic Fluid Management project within the NASA's Exploration Technology Development Program. The authors would like to acknowledge N.T. Van Dresar and G.A. Zimmerli from the NASA Glenn Research Center for providing data on the solubility of helium in liquid oxygen and liquid methane.

This report contains preliminary findings, subject to revision as analysis proceeds.

*Level of Review*: This material has been technically reviewed by technical management.

Available from

NASA Center for Aerospace Information
7115 Standard Drive
Hanover, MD 21076–1320

National Technical Information Service
5285 Port Royal Road
Springfield, VA 22161

Available electronically at http://gltrs.grc.nasa.gov

# Numerical Investigation of LO2 and LCH4 Storage Tanks on the Lunar Surface

Stephen Barsi
National Center for Space Exploration Research
Glenn Research Center
Cleveland, Ohio 44135

Jeff Moder
National Aeronautics and Space Administration
Glenn Research Center
Cleveland, Ohio 44135

Mohammad Kassemi
National Center for Space Exploration Research
Glenn Research Center
Cleveland, Ohio 44135

## Abstract

**Currently NASA is developing technologies to enable human exploration of the lunar surface for durations of up to 210 days. While trade studies are still underway, a cryogenic ascent stage using liquid oxygen (LO2) and liquid methane (LCH4) is being considered for the Altair lunar lander. For a representative Altair cryogenic ascent stage, we present a detailed storage analysis of the LO2 and LCH4 propellant tanks on the lunar surface for durations of up to 210 days. Both the LO2 and LCH4 propellant tanks are assumed to be pressurized with gaseous helium at launch. A two-phase lumped-vapor computational fluid dynamics model has been developed to account for the presense of a non-condensable gas in the ullage. The CFD model is used to simulate the initial pressure response of the propellant tanks while they are subjected to representative heat leak rates on the lunar surface. Once a near stationary state is achieved within the liquid phase, a multi-zone model is used to extrapolate the solution farther in time. For fixed propellant mass and tank size, the long-term pressure response for different helium mass fractions in both the LO2 and LCH4 tanks is examined.**

## Nomenclature

| | | | |
|---|---|---|---|
| $A_i$ | Interfacial area | $\rho$ | Density |
| $C_p$ | Specific heat capacity | $\omega$ | Mass fraction |
| $h$ | Enthalpy / heat transfer coefficient | | Superscripts |
| $\mathbf{j_i}$ | Mass flux | $n$ | Time step number |
| $\mathbf{j_q}$ | Energy flux | $o$ | Initial state |
| $L$ | Latent heat | | Subscripts |
| $m$ | Mass | $g$ | Gas |
| $M$ | Mass transfer rate | $i$,$I$ | Interface |
| $M_g$ | Mass of helium in ullage | $il$ | Liquid side of interface |
| $\mathbf{n}$ | Outward normal | $iv$ | Vapor side of interface |
| $\hat{n}$ | Interfacial normal | $l$ | Liquid |
| $P$ | Pressure | $s$ | Saturation |
| $\mathbf{q}$ | Thermal diffusion flux | $t$ | Tank |
| $\dot{Q}$ | Heat power | $tot$ | Total |
| $R$ | Gas constant | $u$ | Ullage |
| $T$ | Temperature | $v$ | Vapor |
| $\mathbf{v}$ | Velocity | $wl$ | Wall-liquid boundary |
| $V$ | Volume | $wv$ | Wall-vapor boundary |

# I. Introduction

In NASA's current Constellation program, the efficient storage of cryogens has been identified as a core technology.[1] While several propellant changes have occurred within the architecture since the December 2005 release of the Exploration Systems Architecture Study,[1] cryogenic systems are currently envisioned for the Ares-V Earth Departure Stage (EDS) and the Altair lunar lander descent stage. For a representative Altair ascent stage shown in Fig. 1, trades are still underway comparing cryogenic liquid oxygen (LO2) and liquid methane (LCH4) versus hypergolics for use as propellants. For lunar missions, the EDS and Altair cryogenic propellant tanks will be loitering in low Earth orbit (LEO) for days to weeks depending on whether the crew is launched aboard Ares-I before or after Ares-V which contains the lunar lander and the EDS. Additionally, for lunar outpost missions the Altair ascent stage propellant tanks will be required to store cryogens on the lunar surface for up to six months. Such long term storage of cryogens presents a significant challenge. Cryogens are stored at very low temperatures and may be subjected to large heat loads while the tanks are loitering in LEO, in transit, or sitting on the surface of the Moon. When heat leaks into the tank, it will be carried to the liquid-vapor interface by conduction and natural convection. Once this thermal energy reaches the interface, the liquid may start vaporizing. Since vaporization is occurring in a closed tank, the tank pressure will increase.

Various strategies have been identified as possible mechanisms to control tank pressure. The Cryogenic Fluid Management (CFM) project within NASA's Exploration Technology Development Program (ETDP) is investigating many of these pressure control options including subcooled propellant loading prior to launch, using a thermodynamic vent system (TVS), as well as other mixing and cooling devices. In this paper, active pressure control strategies, such as a TVS, are not considered. Rather, we investigate the pressure response of the LO2 and LCH4 ascent tanks on the lunar surface when the tanks are pressurized with a certain amount of gaseous helium (GHe) prior to launch. While the cryogenic ascent tanks may include an active pressure control system, in this paper, we only consider long-duration self-pressurization without any mixing or TVS operation.

For a self-pressurization storage solution, ascent stage LO2 and LCH4 tanks are projected to be approximately 85% full of liquid at launch to accommodate any liquid expansion or pressure rise between launch and ascent from the lunar surface. Also, the ascent engines are currently required to perform abort operations during the lunar descent and this requirement will effect the amount of GHe used to pressurize the ascent propellant tanks at launch. After a successful lunar landing, the LO2 and LCH4 ascent tanks would be required to store LO2 and LCH4 on the lunar surface for up to 210 days before any final GHe pressurization and/or thermal conditioning is necessary to start the ascent engines.

In this paper, we perfrom a detailed storage analysis of representative LO2 and LCH4 ascent tanks on the lunar surface for durations of up to 210 days. While no detailed analysis is performed between launch and lunar landing, representative launch conditions are used to calculate the lunar surface initial conditions. Representative conditions for propellant mass, tank size, tank heat leak, temperature and pressure are based on CFM project estimates. Analysis of the LO2 and LCH4 tanks begin with detailed computational fluid dynamic (CFD) simulations just after lunar landing. The CFD simulations employ a two-phase lumped vapor model[2] where the conservation equations for mass, momentum, and energy are solved in the liquid phase but the ullage is treated as a time-varying but spatially-uniform region where global mass and energy balances are applied. The two-phase lumped vapor model has been extensively used to simulate the self-pressurization and pressure control behavior of both a small-scale hydrogen tank in normal gravity[2] and a large-scale partially full hydrogen tank in a low gravity environment.[3,4] The model has been validated[5] using data from a ground-based experiment[6,7] involving a flightweight partially-full hydrogen tank. For the present analysis, the two-phase lumped vapor model has been extended to include the effects of a non-condensable species in the ullage. Validation of the two-phase lumped vapor model with a non-condensable gas is on-going.

Due to the significant computational overhead of simulating a 210 lunar mission, we use the CFD model to march the solution out for approximately 2 days until a near stationary-state exists in the LO2 and LCH4 tanks. The results are then extrapolated farther in time using a multi-zone model. The long-term pressure response for different helium mass fractions in both the LO2 and LCH4 tanks is examined.

# II. Mathematical Model

## A. Two-Phase Lumped Vapor Model

In what follows, the two-phase lumped vapor model is extended to include the effects of a non-condensable gas in the ullage. The mass of the non-condensable gas in the ullage is assumed constant. Hence, dissolution of the gas into the liquid phase is neglected. Moreover, both the non-condensable and vapor are assumed to behave ideally at the saturation temperature, $T_s$. By Dalton's law of partial pressures, the total pressure in the ullage is

$$P_{tot} = P_v(T_s) + \frac{M_g R_g T_s}{V_v} \tag{1}$$

The ullage is treated as a temporally-varying, spatially-uniform region. Global mass and energy balances are used to couple the lumped ullage model with the transport equations in the liquid. Performing a global mass balance on the ullage yields

$$\frac{d}{dt}(\rho_u V_u) \;=\; -\int \rho_u(\mathbf{v_u} - \mathbf{v_I}) \cdot \hat{n}\, dS \tag{2}$$

where the integration is performed over the liquid-vapor interface and the unit normal vector points into the vapor phase. Expanding eqn. (2) by applying ideal gas mixture relationships yields

$$\frac{d}{dt}(\rho_v V_u + M_g) \;=\; -\int \rho_v(\mathbf{v_v} - \mathbf{v_I}) \cdot \hat{n}\, dS - \int \rho_g(\mathbf{v_g} - \mathbf{v_I}) \cdot \hat{n}\, dS \tag{3}$$

The second term on the left side is zero because the mass of non-condensable in the ullage is assumed to be time-invariant. The second integral on the right side is zero because the gas neither condenses nor dissolves into the liquid phase. Hence,

$$\frac{d}{dt}(\rho_v V_u) \;=\; -\int \rho_v(\mathbf{v_v} - \mathbf{v_I}) \cdot \hat{n}\, dS \;\equiv\; M \tag{4}$$

where, for convenience, we have defined $M$ as the time rate of change of vapor mass in the ullage. As described in Panzarella and Kassemi,[2] we can perform a global mass balance over both the liquid and vapor phases and then integrate the expression in time which results in

$$V_v \;=\; V_v^o \frac{\rho_v^o - \rho_l}{\rho_v - \rho_l} \tag{5}$$

Performing a global energy balance on the ullage yields

$$\frac{d}{dt}\int \rho_u h_u\, dV + \int \rho_u h_u(\mathbf{v_u} - \mathbf{v_I}) \cdot \mathbf{n}\, dS \;=\; -\int \mathbf{j_q} \cdot \mathbf{n}\, dS + \int \frac{dP_{tot}}{dt}\, dV \tag{6}$$

Since two species are present in the ullage, the total energy flux, $\mathbf{j_q}$, is comprised of the heat flux due to thermal diffusion in addition to the heat transported with the mass fluxes:

$$\mathbf{j_q} \;=\; \mathbf{q} + \sum h_i \mathbf{j_i} \tag{7}$$

where the mass flux

$$\mathbf{j_i} \;=\; \rho_i(\mathbf{v_i} - \mathbf{v_u}) \qquad \mathrm{i} = \mathrm{v, g} \tag{8}$$

With some algebra, one can show, after invoking similar assumptions as before, that

$$\int \rho_u h_u(\mathbf{v_u} - \mathbf{v_I}) \cdot \mathbf{n}\, dS = \int \rho_v h_v(\mathbf{v_v} - \mathbf{v_I}) \cdot \mathbf{n}\, dS - \sum \int h_i(\mathbf{j_i} \cdot \mathbf{n})\, dS \tag{9}$$

$$= -M\, h_v - \sum \int h_i(\mathbf{j_i} \cdot \hat{n})\, dS \tag{10}$$

Substituting eqns. (7) and (10) into the global energy balance yields

$$\frac{d}{dt}(\rho_u h_u V_u) - M\, h_v \;=\; \dot{Q}_{wv} + \dot{Q}_{iv} + V_v\left(\frac{dP_v}{dt} + \frac{dP_g}{dt}\right) \tag{11}$$

where $\dot{Q}_{wv}$ and $\dot{Q}_{iv}$ are the heat powers entering the ullage through the wall and through the interface respectively. Applying the energy jump condition

$$M\,L \;=\; \dot{Q}_{il} - \dot{Q}_{iv} \tag{12}$$

to eqn. (11) and simplifying yields

$$\rho_v V_u \frac{dh_v}{dt} + M_g \frac{dh_g}{dt} + \frac{d(\rho_v V_u)}{dt} L - V_v \left( \frac{dP_v}{dt} + \frac{dP_g}{dt} \right) \;=\; \dot{Q}_{wv} + \dot{Q}_{il} \tag{13}$$

or since the ullage is assumed to be thermally uniform at the saturation temperature and both the vapor and gas are ideal

$$\boxed{\frac{dT_s}{dt} \left[ \rho_v V_v C_{p_v} + M_g C_{p_g} + \frac{d(\rho_v V_u)}{dT_s} L - V_v \left( \frac{dP_v}{dT_s} + \frac{dP_g}{dT_s} \right) \right] \;=\; \dot{Q}_{wv} + \dot{Q}_{il}} \tag{14}$$

Equation 14 is an evolution equation for the saturation temperature in the ullage. All terms within the brackets can be evaluated explicitly using thermophysical property data, the saturation curve, ideal gas relationships, and eqn. (5). The heat sources on the right side, $\dot{Q}_{wv}$ and $\dot{Q}_{il}$, are determined from either the boundary condition or the integrated heat flux on the liquid side of the liquid-vapor interface respectively. The latter is evaluated numerically from the computed temperature field in the liquid phase.

In the liquid, since the geometry, boundary conditions, and physics of the problem allow us to exploit symmetry conditions, a 2D axisymmetric representation is employed and the incompressible Reynold's averaged continuity, Navier-Stokes and energy equations are solved along with Menter's shear stress transport $k-\omega$ turbulence equations.[8] In the conservation equations in the liquid, all properties are assumed constant except for density whose variations are accounted for in a Bousinessq body force term in the axial momentum equation. Relevant thermophysical properties used in the lumped vapor formulation are listed in Table 1.

### B. Multi-Zone Model

Due to the computational overhead in obtaining a detailed CFD simulation for a 210 day lunar stay, we instead use the CFD model to march out for two days until a nearly stationary state is established in the tank and then use a multi-zone model to extrapolate the solution out farther in time.

As sketched in Fig. 2, we partition the tank into three zones: a bulk ullage zone, a bulk liquid zone, and an interfacial zone. The interfacial zone is assumed thin and massless and only defined to enforce appropriate jump conditions at the phase boundary. The system of differential equations describing the conservation of mass and energy between the zones is

$$M \;=\; \frac{\dot{Q}_{il} - \dot{Q}_{iv}}{h_v - h_l} \tag{15}$$

$$\frac{dm_v}{dt} \;=\; M \tag{16}$$

$$\frac{dm_l}{dt} \;=\; -M \tag{17}$$

$$m_l \frac{dh_l}{dt} = \dot{Q}_{wl} - \dot{Q}_{il} + (V_t - V_v) \frac{dP_{tot}}{dt} \tag{18}$$

$$(m_v C_{p_v} + M_g C_{p_g}) \frac{dT_v}{dt} = \dot{Q}_{wv} + \dot{Q}_{iv} + V_v \frac{dP_{tot}}{dt} \tag{19}$$

The differential equations are evolved in time using a forward Euler time-stepping routine. The inter-zonal heat transfer terms in eqns. (18) and (19) are computed from

$$\dot{Q}_{il} = h_{il}\, A_i\, (T_l - T_i) \tag{20}$$

$$\dot{Q}_{iv} = h_{iv}\, A_i\, (T_i - T_v) \tag{21}$$

where the heat transfer coefficient, $h$, is evaluating from standard natural convection correlations from horizontal plates.[9] The pressure derivative is evaluated explicitly according to

$$\left( \frac{dP_{tot}}{dt} \right)^n \approx \frac{P_{tot}^n - P_{tot}^{n-1}}{\Delta t} \tag{22}$$

where

$$P_{tot} = \frac{m_v R_v T_v}{V_v} + \frac{M_g R_g T_v}{V_v} \tag{23}$$

Finally, a constitutive model is needed to specify the relationship between the interfacial temperature, the partial pressure of the vapor in the ullage, and the mass transfer rate. We assume that the mass transfer rates in both the LO2 and LCH4 tanks are small enough that, locally, thermodynamic equilibrium exists at the phase boundary. Hence,

$$T_i = T_s(P_v) \tag{24}$$

In the CFD model, constant properties and liquid incompressibility are assumed. Such assumptions are reasonable given that after only two days, the temperature and pressure in the tank have not changed appreciably. Over a 210 day lunar stay however, the temperature and pressure rise in the propellant tanks may be significant. To accommodate these temperature and pressure rises and their corresponding effect on thermophysical properties, in the multi-zone model, properties in both bulk phases are variable. In the ullage, the viscosity and conductivity are evaluated using the following mixing rules:

$$\mu = (1 - \omega_g)\mu_v + \omega_g \mu_g \tag{25}$$

$$k = (1 - \omega_g)k_v + \omega_g k_g \tag{26}$$

Moreover, in the liquid, the incompressibility constraint is relaxed. The liquid density is allowed to vary according to

$$\rho_l \; = \; \rho_l(P_{tot}, h_l) \tag{27}$$

This density functional, as well as other relationships for property variations are taken from NIST RefProp v7.0.

Solution of the zonal model proceeds as follows: First, the temperature of the zones and total pressure inside the tank are initialized using the solution from the detailed CFD model. The interfacial mass transfer rate is computed according the global energy jump condition given by eqn. (15). The global mass balances for the liquid and ullage zones are evolved in time to obtain updated values for the liquid and vapor masses inside the tank. Next, the zonal energy balances are evolved in time resulting in updated values for the liquid enthalpy and ullage temperature. As mentioned before, the liquid incompressibility assumption is relaxed in the multi-zone model. The liquid density is updated iteratively. One guesses a value for the ullage volume at the new time step. With updated values for ullage temperature and vapor mass, and a guessed value for ullage volume, the total pressure can be computed. The updated liquid enthalpy and total pressure are used to evaluate the liquid density according to eqn. (27). The guessed value of the ullage volume is then corrected according to

$$V_v^{n+1} \; = \; V_t - \frac{m_l^{n+1}}{\rho_l^{n+1}} \tag{28}$$

and iteration proceeds until convergence is obtained.

## III. Numerical Implementation

The two-phase lumped vapor model has been implemented into a customized version of the commercial CFD code Fluent. The underlying code solves the continuity, Navier-Stokes, energy conservation, and turbulence equations in the liquid. The interfacial mass transfer model and pressure updating scheme is implemented via user-defined functions.

In the liquid, the flow, energy, and turbulence equations are evolved in time using a backward Euler scheme with a fixed time step of 0.5 s. Spatially, in the momentum, energy, and turbulence equations, second order upwinding is used to discretize the convective fluxes. The SIMPLE method is used to couple the pressure and velocity fields and to enforce continuity. The numerical results were generated on a non-uniform and non-orthogonal mesh of approximately 18000 quadrilateral control volumes with a dense clustering of cells along the tank wall and below the liquid vapor interface. The equations are solved sequentially using a parallel algebraic multigrid solver with a Gauss-Seidel smoother. Convergence is attained within each time step when the L1 norm of the residual for all primary variables falls below $1\times10^{-6}$. It takes approximately 2 weeks of CPU time on 6 AMD 64 bit Opteron processors to march out two days.

The interface is modeled as a stationary slip boundary with a prescribed temperature set equal to the saturation temperature corresponding to the partial pressure of the vapor in the ullage. Within each outer iteration, the interfacial heat power on the liquid side of the interface is computed and used to update the saturation temperature according to eqn. (14). This non-linear evolution equation is updated using a forward Euler time stepping scheme. Once the saturation temperature is updated, the vapor and total pressure in the ullage can be computed and the saturation temperature is prescribed on the phase boundary.

Initially, the liquid in the tank is assumed to be quiescent and isothermal at 92.6 K and 98.1 K for the LO2 and LCH4 tanks respectively. Moreover, the incident heat load is assumed to be distributed uniformly around the tank wall.

## IV. Discussion

Two different lunar surface initial conditions are analyzed in detail for the spherical LO2 and LCH4 tanks. Initial conditions at the lunar surface are determined from the launch conditions assuming no venting and no additional GHe is added to the propellant tanks between launch and lunar landing. At launch, the LO2 and LCH4 tanks are assumed to be 85% full at 90.6 K and 96.1 K respectively. For both propellant tanks, we analyze the self-pressurization behavior when the tanks are pressurized at launch with GHe to either 100 psi or 200 psi. While loitering in LEO, in transit, and descending to the lunar surface, we allow for some heat leak into the tanks and assume the average temperatures in the LO2 and LCH4 tanks after lunar landing have risen to 92.6 K and 98.1 K respectively. This 2 K rise in average propellant temperature from launch to lunar landing is a conservative estimate of temperature rise based on the largest values from CFM projects estimates. Moreover, we assume that after landing on the Moon, the liquid propellants are initially in thermodynamic equilibrium with their saturated vapors. Heat loads for LO2 and LCH4 tanks are provided by CFM project estimates for a south pole location and include a 50% margin.

Representative thermal and flow fields for the LO2 tank initially pressurized to 100 psi are shown in Fig.3 (thermal flow fields for 200 psi launch are similar, but not shown). The LO2 tank is subjected to a heat load of 4 W distributed uniformly around the tank wall. In the lunar gravity field, the incident heat load results in natural convection vortices along the tank wall which carry this incident energy up to the liquid-vapor interface. As the liquid vaporizes, both the vapor pressure and partial pressure of helium increase. Thermodynamically, assuming local equilibrium at the phase boundary, an increase in the vapor pressure of LO2 will cause the interfacial temperature to rise. As indicated in Fig. 3a, the interfacial temperature rises faster than the bulk liquid temperature which results in a stable thermal stratification below the liquid-vapor interface. The stratification is more apparent in Fig. 3c where the temperature field at time = 2 days is shown. The stable stratification below the interface is reducing the extent of the natural convection vortices along the tank's side wall as indicated in Fig. 3d.

A time history of the total ullage pressure corresponding to this case is shown in Fig. 4 where one finds that the total pressure has risen 1.55 psi after the tank had been self-pressurizing for two days. Initially the pressurization rate is non-uniform owing to the developing thermal gradients and flow field within the bulk liquid. After approximately 20 hours, the pressurization rate becomes linear which is indicative of a near stationary state in the tank.

A time history of the partial pressure contributions to the total pressure, shown in Fig. 4b, reveals that both the vapor pressure and partial pressure of helium rise during the two days of self-pressurization. Because the heat load is uniformly distributed around the tank wall, a portion of the incident energy directly enters the ullage and causes the ullage temperature to rise. Moreover, mass transfer into the ullage through the liquid-vapor interface causes the mass of vapor and ullage volume to change. Since both the oxygen vapor and GHe are treated as ideal gases:

$$\Delta P_v = R_v \Delta\left(\frac{m_v\, T_v}{V_v}\right) \tag{29}$$

$$\Delta P_g = M_g\, R_g \Delta\left(\frac{T_v}{V_v}\right) \tag{30}$$

where we note again the mass of GHe in the ullage is assumed constant for the present analysis. Because the change in ullage volume is negligible ($< 0.03\%$) over the two day period of self-pressurization, the change in the partial pressure of helium is primarily due to an increase in the ullage temperature resulting from the incident heat load. The vapor pressure of oxygen increases faster than the partial pressure of helium

because in addition to the thermal contribution to the pressure rise, liquid vaporization at the interface also leads to a rise in tank pressure. When the LO2 tank is pressurized at launch to 100 psi, after two days, the rise in vapor pressure and partial pressure of helium are 1.04 psi and 0.55 psi respectively. When the tank is initially pressurized to 200 psi, the rise in vapor pressure and helium pressure is 1.02 psi and 1.11 psi respectively. The addition of more GHe in the ullage has a negligible effect on the vapor pressure rise. However, as suggested by eqn. (30), increasing the amount of helium in the ullage will result in a larger rise in the partial pressure of GHe. Consequently, the total pressure rise is greater in the LO2 tank initially pressurized to 200 psi than when the tank is pressurized to 100 psi.

To gage the amount of thermal stratification in the LO2 tank, a time history of the minimum and maximum temperatures in the liquid is shown in Fig. 5. For the first 2.5 hours, some noise is apparent in the temperature histories. During this time, flow in the liquid is transitioning from laminar to turbulent natural convection. After 2.5 hours, the noise has decayed and smooth temperature histories are observed. The maximum temperature in the liquid occurs at the liquid-vapor interface and because of thermal stratification, colder fluid has settled to the bottom of the tank. After self-pressurizing for two days, the maximum $\Delta$T in the liquid is 0.36 K.

After marching the solution out two days, the CFD analysis is stopped and the resulting numerical solution is used to initialize the multizone tank model. Specifically, the average temperature in the bulk liquid, the saturation temperature, the total ullage pressure, the vapor mass, and the ullage volume are extracted from the numerical results and used to initialize the multizone formulation. When beginning the multizone analysis, a small jump in ullage pressure is observed. The jump is less than 1 psi and decays after several time steps. A small jump is not surprising given that the solution is transitioning between two different pressurization models – from an incompressible liquid and saturated vapor CFD model to an analytical model that relaxes several of these constraints.

The multizone pressurization model continues to track the total ullage pressure for up to 210 days. For the LO2 tank, the analysis is terminated when either the total pressure reaches 375 psi or the liquid temperature reaches 127 K. When either of these conditions are reached, it is envisioned that some pressure control strategy would be employed to reduce the ullage pressure and/or cool the bulk liquid. The implementation of a particular pressure reduction strategy (i.e. venting) is beyond the scope of the current paper but will be analyzed in the future.

The long term pressure and temperature history for the LO2 tank is shown in Fig. 6 with further details provided in Table 3. The pressure histories reveal that the LO2 tank, initially at 200 psi, should be vented after 103 days on the lunar surface, while the tank initially at 100 psi can remain on the lunar surface for an additional 79 days before venting is required. As indicated in Table 3, the temperature in the liquid is below the limiting value of 127 K when venting commences. Furthermore, Fig. 6b indicates that the liquid temperature rise rate is insensitive to pressure variation. Thus, even after several cycles of venting and pressure rise back to 375 psi, it is a reasonable to expect that the liquid temperature rise rate will remain constant out to 210 days. Using the liquid temperature rise rate value when venting first occurs (0.0047 K/hr) predicts the LO2 tank average liquid temperature after 210 days of lunar surface storage of 115.88 K for 100 psi launch and 116.19 K for 200 psi launch.

Similar results are observed for the self-pressurizing LCH4 tanks. Thermal and flow fields at different instants in time are shown in Fig. 7 where after six hours, primary natural convection vortices in the bulk liquid have developed along the tank wall. Secondary vortices, driven by buoyantly rising plumes from the bottom of the tank are also observed. As in the LO2 tank, the thermal field in the LCH4 tank is stably stratifying which weakens the natural convection vortices in the bulk liquid.

The total pressure history for the LCH4 tank initially pressurized to 100 psi is shown in Fig. 8a. After self-pressurizing for two days, the ullage pressure has only risen 0.62 psi. This pressure rise is smaller than the corresponding rise in the LO2 tank but expected since the incident heat load is halved. The partial pressure histories, shown in Fig. 8b, reveal that the vapor pressure and partial pressure of helium have risen 0.19 psi and 0.43 psi respectively. Thus, in contrast to the LO2 tank, the partial pressure of helium has risen faster than the vapor. As indicated in Table 2, for the methane tanks, the initial mass fraction of GHe in the ullage is significantly larger than the initial helium mass fraction in the LO2 tanks. Additionally, the latent heat of methane is larger than the latent heat of oxygen at these operating conditions which indicates that more energy is required to vaporize the liquid and consequently the vaporization rate is smaller in the LCH4 tanks than in the LO2 tanks. The combined effect of a smaller vapor mass and decreased vaporization rate leads to a vapor pressure rise smaller than the partial pressure rise of GHe.

When the LCH4 tank is initially pressurized to 200 psi, the vapor pressure and partial pressure of GHe have risen to 0.19 psi and 0.87 psi respectively. Similar to the LO2 tank, the additional helium in the ullage at 200 psi has a negligible effect on the vapor pressure rise but has nearly doubled the the pressure rise of GHe. Consequently, the total pressure rise for the methane tank at 200 psi is greater than when the tank is initially pressurized to 100 psi.

To gage the thermal stratification in the liquid, the minimum and maximum temperature histories are shown in Fig. 9 where one finds after self-pressurizing for two days, the maximum $\Delta$T in the bulk liquid is 0.29 K - smaller than the LO2 tank because the applied heat load is reduced.

The long term pressure and temperature behavior resulting from the multizone analysis is shown in Fig. 10 with further details provided in Table 3. The multizone model tracks the ullage pressure until either the total pressure reaches 375 psi or the liquid temperature reaches 158 K after which venting or another pressure control strategy would be required to reduce ullage pressure and/or cool the bulk liquid. As indicated in Fig. 10a, for the methane tanks initially pressurized to 200 psi, venting would be required after 203 days. When the tanks are initially pressurized to 100 psi, they can remain on the lunar surface for a full 210 day mission without venting as both the final liquid temperature and ullage pressure are well within the design limits. Fig. 10b indicates that the liquid temperature rise rate is insensitive to pressure variation, as was the case for the LO2 tanks. By the same reasoning as used in analysis of the LO2, it is reasonable to assume the liquid temperature rise rate will not be significantly effected by venting and pressure rise cycles. Thus, for the 200 psi launch case, the LCH4 tank liquid temperature after 210 days of lunar surface storage is approximated as 115.62 K assuming a constant liquid temperature rise rate value of 0.0035 K/hr.

## V. Conclusions

In this paper, a detailed storage tank analysis is performed to analyze the self-pressurization behavior of LO2 and LCH4 tanks on the lunar surface. The propellant tanks are pressurized with GHe prior to launch and subjected to heat leaks, temperature, and pressure conditions on the lunar surface representative of a cryogenic ascent stage. Conservative (i.e., large) values taken from CFM project studies are used for for heat leaks, tank sizes and the propellant temperature increase from launch to lunar landing. Also, the lack of any mixing (such as an axial jet to promote bulk liquid mixing) during the 210 day lunar storage allows for the maximum degree of thermal stratification and thus represents a somewhat worse-case scenario for lunar surface cryogenic storage. The analysis performed is applicable to a long duration lunar outpost mission with a nominal duration of 180 days and a maximum duration of 210 days.

Analysis of the storage tanks begins with detailed CFD simulations. Computationally, a two-phase lumped vapor model has been extended to include the effects of a non-condensable gas in the ullage. After marching out two days in simulation time, results from the CFD solution are used to initialize a multizone model which carries the solution out farther in time for up to 210 days. The multizone analysis is terminated if maximum pressure or maximum liquid temperature conditions are reached. For the cases simulated, maximum liquid temperature conditions are not encountered, while some cases do encounter the maximum pressure condition of 375 psi. A simple ullage vent system could reduce tank pressure when the maximum pressure condition is reached. While ullage venting is not analyzed in this study, the insensitivity of the average liquid temperature rise rate to pressure variations (as shown in Figs. 6b and 10b) does allow using the results of this study to extrapolate the liquid temperature out to 210 days of lunar storage, even if several venting cycles were to occur between the end of the multizone analysis and 210 days storage. Such extrapolation of liquid temperature shows that both LO2 and LCH4 tanks are unlikely to require thermal conditioning (such as operating an axial jet TVS) over a 210 days of lunar surface storage to meet engine inlet start conditions currently anticipated for lunar ascent.

For both the LO2 and LCH4 tanks, when pressurized to 200 psi at launch, the total ullage pressure rises faster than if the tanks were pressurized to 100 psi. For LO2 tanks pressurized with GHe to 200 psi at launch and a lunar surface heat load of 4 W, venting would be required after 103 days of lunar surface storage while LO2 tanks pressurized to 100 psi at launch require venting at 182 days. Because of a smaller incident heat load, the ullage pressure rises more slowly in the LCH4 tanks than in the LO2 tanks. For LCH4 tanks pressurized with GHe to 200 psi at launch and a lunar surface heat load of 2 W, venting would be required after 203 days of lunar surface storage, while LCH4 tanks pressurized to 100 psi at launch do not require venting over the entire 210 days of lunar surface storage. No thermal conditioning appears to be required for any cases analyzed over the entire 210 days of lunar surface storage. Operation of a mixing

device (such as axial jet bulk liquid mixer) would most likely provide longer storage duration before ullage venting was required compared to the predictions presented in this paper.

## References


[1]NASA Exploration Systems Architecture Study. NASA TM-2005-214062, 2005.

[2]C. H. Panzarella and M. Kassemi. On the validity of purely thermodynamic descriptions of two-phase cryogenic fluid storage. J. Fluid Mech., 484:41–68, 2003.

[3]C. H. Panzarella and M. Kassemi. Self-pressurization of large spherical cryogenic tanks in space. J. Spacecraft and Rockets, 42:299–308, 2005.

[4]C. Panzarella, D. Plachta, and M. Kassemi. Pressure control of large cryogenic tanks in microgravity. Cryogenics, 44:475–483, 2004.

[5]S. Barsi and M. Kassemi. Numerical and experimental comparisons of the self-pressurization behavior of an LH2 tank in normal gravity. Cryogenics, 48(3/4):122–129, 2008.

[6]N. T. Van Dresar, C. S. Lin, and M. M. Hasan. Self-pressurization of a flightweight liquid hydrogen tank: Effects of fill level at low wall heat flux. Technical Report 105411, NASA Tech. Mem., 1992.

[7]M.M. Hasan, C.S. Lin, and N.T. Van Dresar. Self-pressurization of a flightweight liquid hydrogen storage tank subjected to low heat flux. NASA TM 103804, 1991.

[8]F.R. Menter. Zonal two-equation k-w turbulence models for aerodynamic flows. AIAA 93-2906, 1993.

[9]F.P. Incropera and D.P. DeWitt. Fundamentals of Heat and Mass Trnasfer. Wiley, 3rd edition, 1990.


| Property | LO2 | LCH4 |
|---|---|---|
| Liquid Density | 1130.6 kg $m^{-3}$ | 442.0 kg $m^{-3}$ |
| Liquid Specific Heat | 1703.0 J $kg^{-1}$ $K^{-1}$ | 3393.7 J $kg^{-1}$ $K^{-1}$ |
| Liquid Conductivity | 0.148 W $m^{-1}$ $K^{-1}$ | 0.203 W $m^{-1}$ $K^{-1}$ |
| Liquid Viscosity | $1.84\times10^{-4}$ Pa s | $1.60\times10^{-4}$ Pa s |
| Liquid Expansion Coef. | 0.00445 $K^{-1}$ | 0.00308 $K^{-1}$ |

**Table 1. Some thermophysical properties of LO2 and LCH4.**

| Condition | LO2 | | LCH4 | |
|---|---|---|---|---|
| $P_{tot}$ at launch | 100 psi | 200 psi | 100 psi | 200 psi |
| Propellant Mass (Liquid + Vapor) | 1840.5 kg | 1840.5 kg | 613.5 kg | 613.5 kg |
| Tank Volume | 1.897 $m^3$ | 1.897 $m^3$ | 1.623 $m^3$ | 1.623 $m^3$ |
| T at launch | 90.6 K | 90.6 K | 96.1 K | 96.1 K |
| T after lunar landing | 92.6 K | 92.6 K | 98.1 K | 98.1 K |
| Helium mass | 0.8826 kg | 1.9391 kg | 0.8133 kg | 1.6643 kg |
| Initial vapor mass | 0.9243 kg | 1.469 kg | 0.1318 kg | 0.1308 kg |
| Initial helium mass fraction | 0.49 | 0.57 | 0.86 | 0.93 |
| $P_{tot}$ after lunar landing | 109.77 psi | 216.94 psi | 106.31 psi | 211.84 psi |
| Fill level after lunar landing | 85.74% | 85.61% | 85.51% | 85.41% |
| Net Heat Load | 4 W | 4 W | 2 W | 2 W |

**Table 2. Representative case studies being analyzed.**

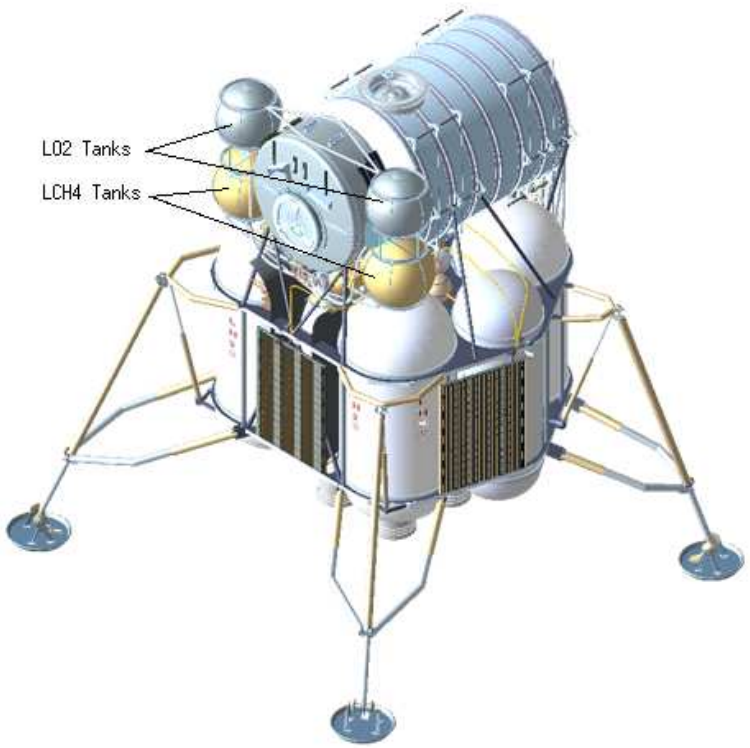


**Figure 1. LO2 and LCH4 tanks on a representative lunar lander.**

LCH4 initially at 100 psi

| Time | $T_l$ [K] | $T_u$ [K] | $P_{tot}$ [psia] | Fill Fraction | $\frac{dP_{tot}}{dt}$ [psi/hr] | $\frac{dT}{dt}$ [K/hr] |
|---|---|---|---|---|---|---|
| 30 days | 100.59 | 100.93 | 115.46 | 0.862 | 0.013 | 0.0035 |
| 60 days | 103.08 | 103.39 | 125.35 | 0.868 | 0.015 | 0.0035 |
| 90 days | 105.56 | 105.85 | 136.58 | 0.875 | 0.017 | 0.0035 |
| 180 days | 112.96 | 113.20 | 181.28 | 0.896 | 0.026 | 0.0034 |
| 210 days | 115.42 | 115.65 | 201.28 | 0.904 | 0.030 | 0.0034 |

LCH4 initially at 200 psi

| Time | $T_l$ [K] | $T_u$ [K] | $P_{tot}$ [psia] | Fill Fraction | $\frac{dP_{tot}}{dt}$ [psi/hr] | $\frac{dT}{dt}$ [K/hr] |
|---|---|---|---|---|---|---|
| 30 days | 100.60 | 100.93 | 228.89 | 0.861 | 0.024 | 0.0035 |
| 60 days | 103.11 | 103.41 | 247.17 | 0.867 | 0.027 | 0.0035 |
| 90 days | 105.61 | 105.89 | 267.75 | 0.874 | 0.030 | 0.0035 |
| 180 days | 113.10 | 113.33 | 348.34 | 0.894 | 0.046 | 0.0035 |
| 202.9 days | 115.01 | 115.23 | 375.00 | 0.900 | 0.051 | 0.0035 |
| 210 days* | 115.62 | | | | | |

LO2 initially at 100 psi

| Time | $T_l$ [K] | $T_u$ [K] | $P_{tot}$ [psia] | Fill Fraction | $\frac{dP_{tot}}{dt}$ [psi/hr] | $\frac{dT}{dt}$ [K/hr] |
|---|---|---|---|---|---|---|
| 30 days | 95.92 | 96.30 | 129.64 | 0.870 | 0.030 | 0.0046 |
| 60 days | 99.22 | 99.58 | 154.01 | 0.883 | 0.038 | 0.0046 |
| 90 days | 102.52 | 102.86 | 185.22 | 0.897 | 0.049 | 0.0046 |
| 180 days | 112.50 | 112.76 | 366.46 | 0.942 | 0.145 | 0.0048 |
| 182.4 days | 112.78 | 113.03 | 375.00 | 0.942 | 0.151 | 0.0047 |
| 210 days* | 115.88 | | | | | |

LO2 initially at 200 psi

| Time | $T_l$ [K] | $T_u$ [K] | $P_{tot}$ [psia] | Fill Fraction | $\frac{dP_{tot}}{dt}$ [psi/hr] | $\frac{dT}{dt}$ [K/hr] |
|---|---|---|---|---|---|---|
| 30 days | 95.94 | 96.27 | 251.19 | 0.868 | 0.052 | 0.0046 |
| 60 days | 99.29 | 99.60 | 293.13 | 0.881 | 0.065 | 0.0046 |
| 90 days | 102.65 | 102.93 | 346.78 | 0.895 | 0.085 | 0.0047 |
| 103.0 days | 104.11 | 104.39 | 375.00 | 0.901 | 0.096 | 0.0047 |
| 180 days* | 112.80 | | | | | |
| 210 days* | 116.19 | | | | | |

**Table 3. Summary of results from the multizone model. (*Extrapolated using constant $dT_l/dt$)**

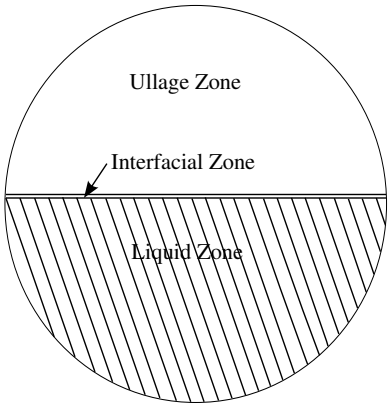


**Figure 2. Sketch of the three zones used in the multi-zone model.**

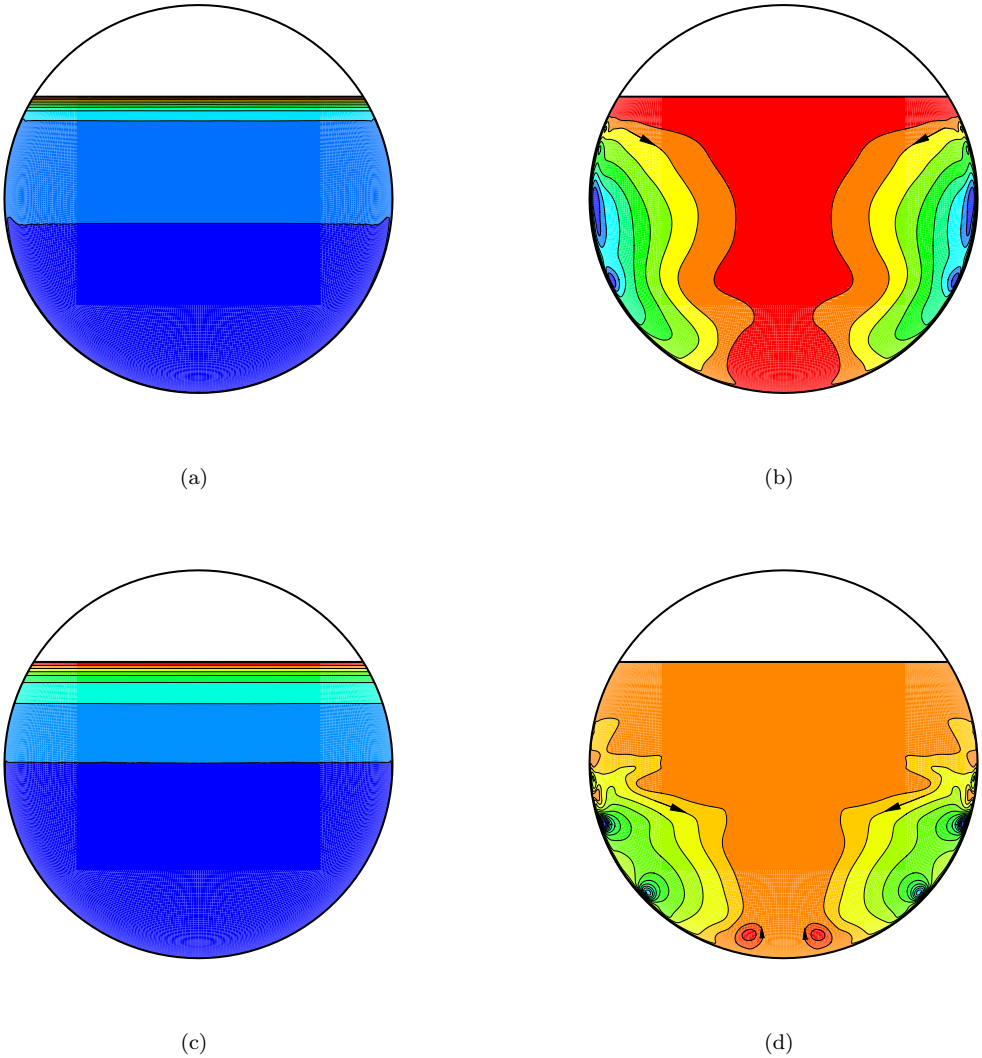

(a) (b)

(c) (d)

**Figure 3. Temperature (a) and Flow field (b) at time = 6 hours for the LO2 tank. ($T_{min}$= 92.61 K, $T_{max}$= 92.79 K, $\|v\|_{max}$= 2.61 mm/s). Temperature (c) and Flow field (d) at time = 2 days for the LO2 tank. ($T_{min}$= 92.77 K, $T_{max}$= 93.14 K, $\|v\|_{max}$= 2.62 mm/s).**

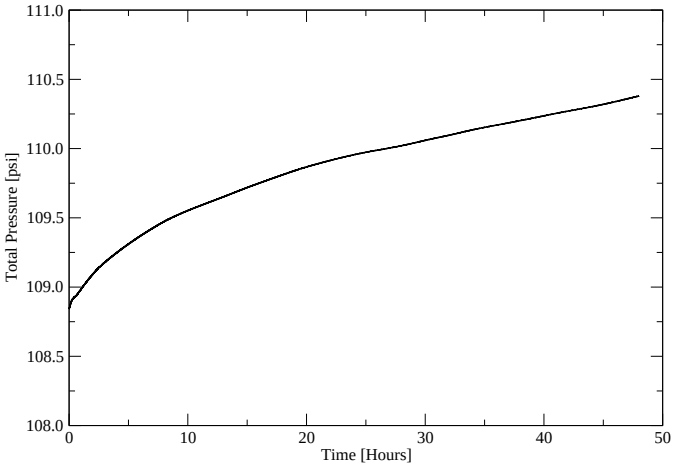


(a)

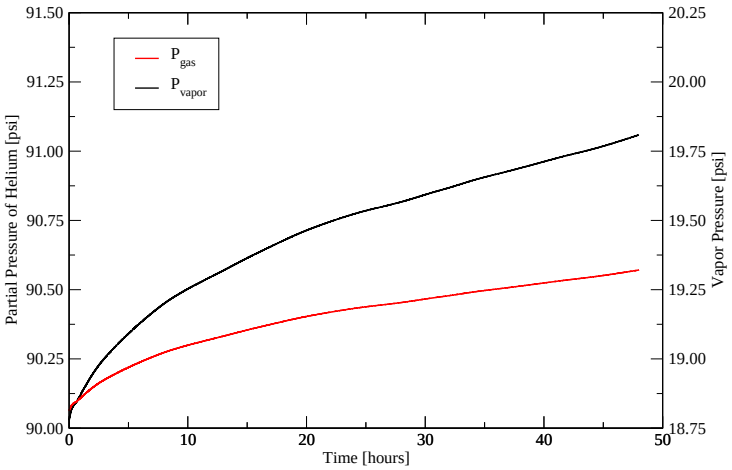


(b)

**Figure 4. Total pressure and partial pressure histories in the LO2 tank during two days of self-pressurization. (Initial launch pressure = 100 psi)**

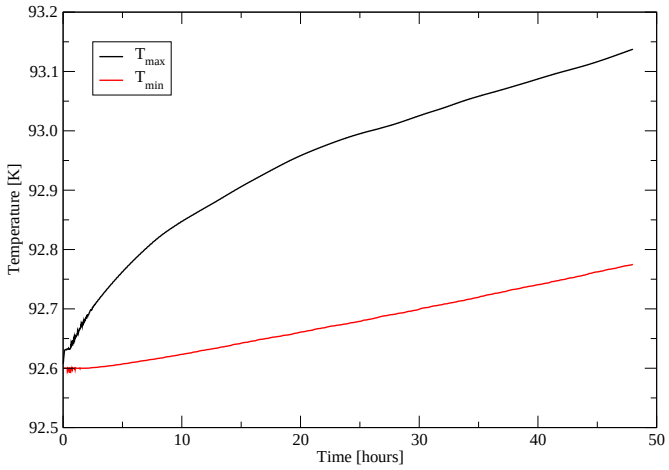


**Figure 5. Minimum and maximum liquid temperatures in the LO2 tank. (Initial launch pressure = 100 psi)**

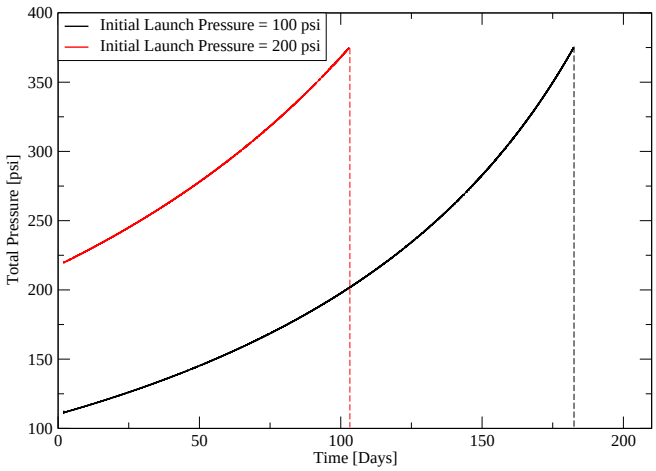


(a)

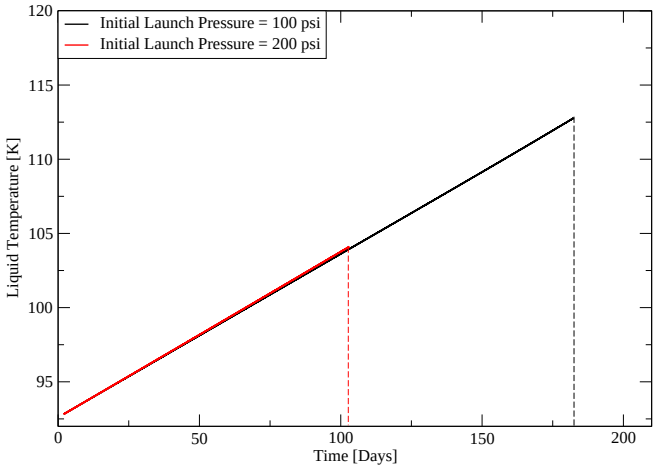


(b)

**Figure 6. Long term pressure (a) and temperature (b) behavior in the LO2 tank.**

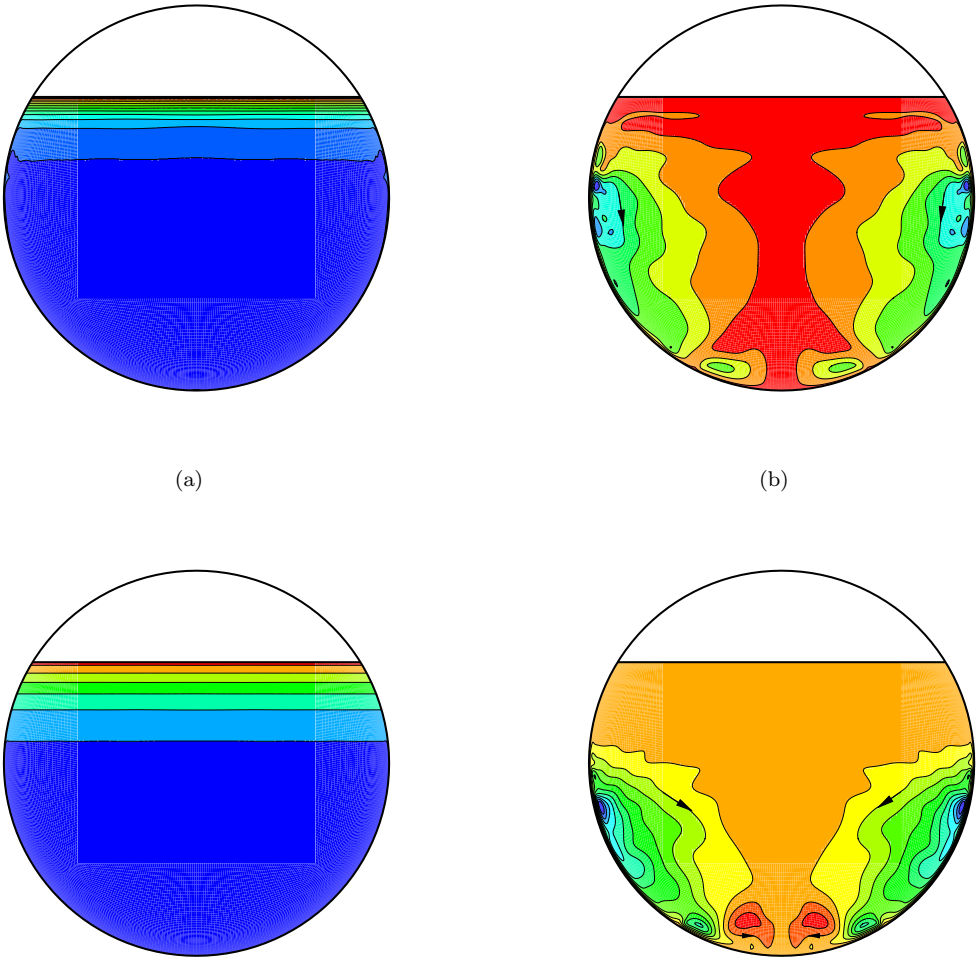

(a) (b)

(c) (d)

**Figure 7. Temperature (a) and Flow field (b) at time = 6 hours for the LCH4 tank. ($T_{min}$= 98.11 K, $T_{max}$= 98.23 K, $\|v\|_{max}$= 1.51 mm/s). Temperature (c) and Flow field (d) at time = 2 days for the LCH4 tank. ($T_{min}$= 98.22 K, $T_{max}$= 98.52 K, $\|v\|_{max}$= 1.13 mm/s).**

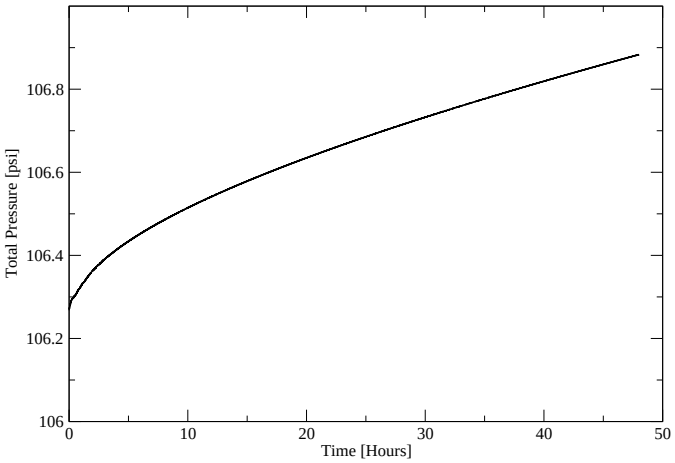


(a)

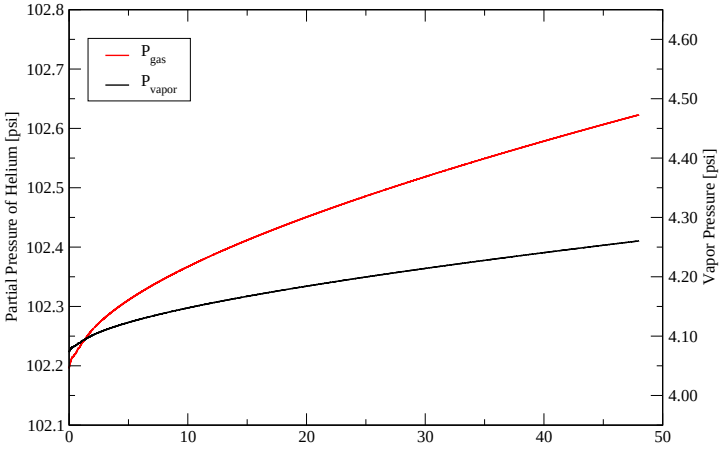


(b)

**Figure 8. Total pressure and partial pressure histories in the LCH4 tank during two days of self-pressurization. (Initial launch pressure = 100 psi)**

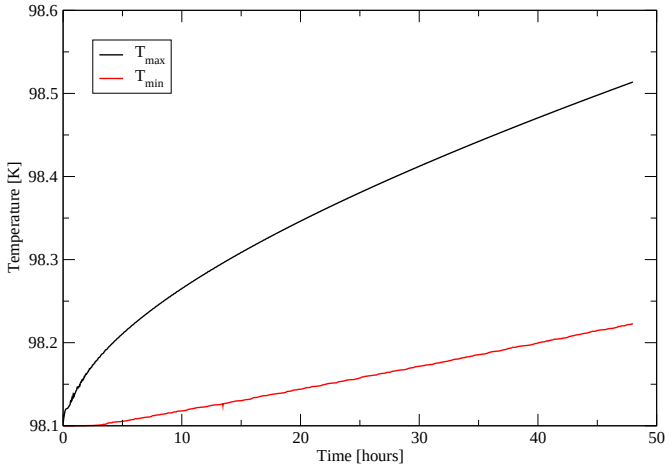


**Figure 9. Minimum and maximum liquid temperatures in the LCH4 tank. (Initial launch pressure = 100 psi)**

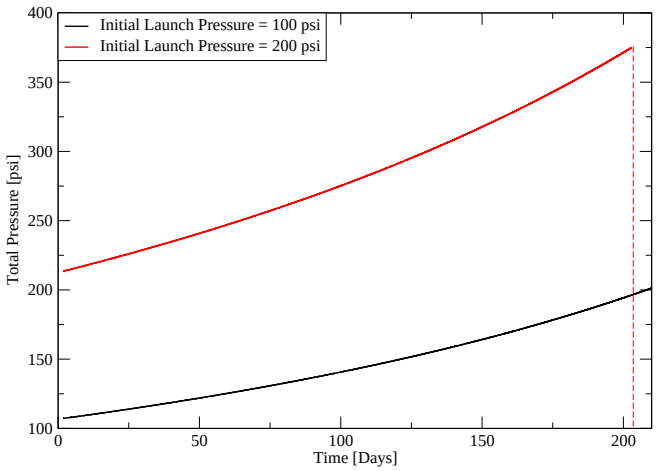


(a)

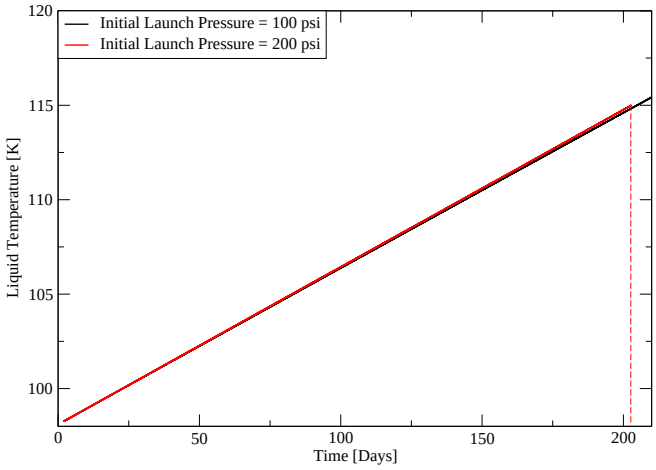


(b)

**Figure 10. Long term pressure (a) and temperature (b) behavior in the LCH4 tank.**

| REPORT DOCUMENTATION PAGE | Form Approved OMB No. 0704-0188 |
|---|---|



| 1. REPORT DATE *(DD-MM-YYYY)* | 2. REPORT TYPE | 3. DATES COVERED *(From - To)* |
|---|---|---|
| 01-12-2008 | Technical Memorandum | |

**4. TITLE AND SUBTITLE**
Numerical Investigation of LO2 and LCH4 Storage Tanks on the Lunar Surface

**5a. CONTRACT NUMBER**

**5b. GRANT NUMBER**

**5c. PROGRAM ELEMENT NUMBER**

**6. AUTHOR(S)**
Barsi, Stephen; Moder, Jeff; Kassemi, Mohammad

**5d. PROJECT NUMBER**

**5e. TASK NUMBER**

**5f. WORK UNIT NUMBER**
WBS 095240.04.03.01.04.03

**7. PERFORMING ORGANIZATION NAME(S) AND ADDRESS(ES)**
National Aeronautics and Space Administration
John H. Glenn Research Center at Lewis Field
Cleveland, Ohio 44135-3191

**8. PERFORMING ORGANIZATION REPORT NUMBER**
E-16641

**9. SPONSORING/MONITORING AGENCY NAME(S) AND ADDRESS(ES)**
National Aeronautics and Space Administration
Washington, DC 20546-0001

**10. SPONSORING/MONITORS ACRONYM(S)**
NASA; AIAA

**11. SPONSORING/MONITORING REPORT NUMBER**
NASA/TM-2008-215443; AIAA-2008-4749

**12. DISTRIBUTION/AVAILABILITY STATEMENT**
Unclassified-Unlimited
Subject Categories: 20 and 28
Available electronically at http://gltrs.grc.nasa.gov
This publication is available from the NASA Center for AeroSpace Information, 301-621-0390

**13. SUPPLEMENTARY NOTES**

**14. ABSTRACT**
Currently NASA is developing technologies to enable human exploration of the lunar surface for duration of up to 210 days. While trade studies are still underway, a cryogenic ascent stage using liquid oxygen (LO2) and liquid methane (LCH4) is being considered for the Altair lunar lander. For a representative Altair cryogenic ascent stage, we present a detailed storage analysis of the LO2 and LCH4 propellant tanks on the lunar surface for durations of up to 210 days. Both the LO2 and LCH4 propellant tanks are assumed to be pressurized with gaseous helium at launch. A two-phase lumped-vapor computational fluid dynamics model has been developed to account for the presense of a noncondensable gas in the ullage. The CFD model is used to simulate the initial pressure response of the propellant tanks while they are subjected to representative heat leak rates on the lunar surface. Once a near stationary state is achieved within the liquid phase, multizone model is used to extrapolate the solution farther in time. For fixed propellant mass and tank size, the long-term pressure response for different helium mass fractions in both the LO2 and LCH4 tanks is examined.

**15. SUBJECT TERMS**
Cryogenic storage; Lunar surface; Computational fluid dynamics

| 16. SECURITY CLASSIFICATION OF: | | | 17. LIMITATION OF ABSTRACT | 18. NUMBER OF PAGES | 19a. NAME OF RESPONSIBLE PERSON |
|---|---|---|---|---|---|
| a. REPORT | b. ABSTRACT | c. THIS PAGE | | | STI Help Desk (email:help@sti.nasa.gov) |
| U | U | U | UU | 25 | 19b. TELEPHONE NUMBER *(include area code)* 301-621-0390 |